== ATOMS, MOLECULES, OPTICS ==

OPTICAL STABILIZATION OF CHARGED DIELECTRIC NANOPARTICLES IN HYBRID TRAPS

© 2024 E. V. Soboleva*, D. P. Shcherbinin, S. S. Rudyi, and A. V. Ivanov

International Research and Educational Center for Physics of Nanostructures, ITMO University, Saint Petersburg, 197101 Russia

*e-mail: eliz.sobol239@gmail.com

Received April 03, 2024 Revised April 30, 2024 Accepted May 06, 2024

Abstract. The results of a theoretical study of the dynamics of charged dielectric nanoparticles in a hybrid trap are presented. A new configuration of a hybrid trap is proposed, consisting of a surface electrodynamic trap with transparent electrodes and an optical dipole trap formed by a laser Gaussian beam. Dynamics simulation was carried out for silicon dioxide nanoparticles localized in a hybrid trap in an air environment, taking into account viscous friction. It is shown that the laser radiation intensity of the dipole trap can be used as a bifurcation parameter of the considered dynamical system to change the equilibrium position of nanoparticles. The proposed hybrid trap configuration can become a new platform for implementing an optomechanical Ising machine.

The article is presented as part of the publication of conference materials "Physics of Ultracold Atoms" (PUCA-2023), Novosibirsk, December 2023.

DOI: 10.31857/S0044451024100092

1. INTRODUCTION

Hybrid traps that combine electrodynamic and optical capture and confinement methods in one device open up wide possibilities for localization and control of single micro- and nanoparticles. The main feature of hybrid traps is the ability to localize particles at different spatial scales. For example, the localization area width of electrodynamic traps usually takes a value in the range from several nanometers to several centimeters. In contrast, the potential well width of an optical tweezers is characterized by the Gaussian beam width and usually amounts to up to $10 \mu m [1-3]$, with a potential depth exceeding the electrodynamic trap potential by several orders of magnitude [4]. Thus, localization is carried out using a two-stage approach: at the first stage, coarse localization of charged particles occurs in the electrodynamic trap field, and at the second stage, fine localization is performed in the optical tweezers field.

Usually, quadrupole radiofrequency traps or other trap configurations with a single stable equilibrium position for charged particles are used to create hybrid traps [4–7]. This choice determines the effective coupling of coordinate potentials for electrodynamic and optical minima. However, this potential distribution is not the only possible one. For example, surface electrodynamic traps are known where the formation of multiple equilibrium positions is observed [8–10]. At the same time, several stable equilibrium points in an optical tweezers can be realized using Hermite-Gauss beams in higher-order modes [2, 11].

From a practical point of view, the implementation of a hybrid trap where one of the potentials is characterized by multiple equilibrium positions may be interesting It can be assumed that in such systems, the effect of equilibrium position bifurcation may be observed when changing the ratio of control parameters. Physically, this means that with one set of control parameters, retention will be almost completely determined by interaction with the electrodynamic trap potential, and when parameters change, by the optical tweezers potential. Thus, the

position and number of stable equilibrium points will be uniquely determined by the ratio of control parameters in the hybrid system.

The presence of a bifurcation point in the studied system opens up the possibility of physical implementation of the Ising machine [12], which represents a new type of computational device based on a non-von Neumann architecture, specializing in efficiently solving combinatorial optimization problems [13]. Depending on the value of the control parameter in a system with a bifurcation point, there is either one stationary state or two. In the vicinity of the bifurcation point, the system dynamics become unstable, and there is uncertainty in the transition of the system to one of two stationary states. Such system behavior can be used for encoding spin states of the Ising model [14]. Physical systems that can obtain solutions to the Ising model have the potential for practical application in solving optimization problems in various areas of human activity [14, 15]. Previously, it was shown that coupled optical parametric oscillators [16], Kerr cells [17], Josephson oscillators [18], and other nonlinear dynamic systems can be used as a platform for implementing the Ising machine. Using the proposed hybrid trap as a new platform for implementing the Ising machine appears to be a promising research direction.

In this work, a new configuration of a hybrid trap is proposed, consisting of a surface electrodynamic trap with transparent electrodes and an optical dipole trap. It should be noted that the use of transparent electrodes in the electrodynamic trap allows positioning the laser beam of the optical trap vertically, which distinguishes the proposed hybrid trap configuration from other used configurations and determines the results obtained in this work. It is shown that during the localization of nanoparticles in the surface trap, the formation of two stable equilibrium positions is observed, caused by the destruction of the symmetry of the effective potential. At laser radiation intensity values where the gradient force exceeds the interaction forces of particles with the electric field of the trap, a transition of the system to a dynamic mode characterized by one stable localization point is observed. Thus, it is shown that control of the particle position in the hybrid trap can be achieved solely by changing the laser radiation intensity, without any changes in the radiation propagation direction or without changing the mutual arrangement of the trap elements.

2. MATHEMATICAL MODEL OF A HYBRID TRAP

To describe the dynamics of nanoparticles in hybrid traps, the following approximations are used. First, the interaction of optical radiation with the localization object is described within the dipole approximation, where the size of the localization object is significantly smaller than the wavelength of laser radiation. In this work, we consider silicon dioxide nanoparticles with a hydrodynamic radius of a = 20 nm. It should be noted that the dipole approximation in modeling the interaction of silicon dioxide particles with laser radiation at a wavelength of 1064 nm can be applied to particles with a characteristic size of no more than $\sim \lambda / 10$ nm. For example, the extinction cross-section for silicon dioxide nanoparticles with a size of 20 nm, determined in the dipole approximation [2], is $4.70 \cdot 10^{-2}$ nm² within the Mie scattering theory $4.89 \cdot 10^{-2}$ nm² [19]. As the particle size increases, it is necessary to take into account the excitation of quadrupole moments and higher-order moments or use Mie theory. In addition, the scattering crosssection can be estimated experimentally, as in work [20]. Second, a spherical approximation of the localization object shape is used in dynamic analysis, which allows describing energy dissipation during localization in air within the Stokes approximation. Third, the spatial distribution of the potential was evaluated by solving the Dirichlet problem for the upper half-space (z > 0).

To implement the electrodynamic module of the hybrid trap, a surface electrodynamic trap is used in the configuration proposed in work [21]. The scheme of the electrodynamic trap is shown in Fig. 1. In essence, the electrodynamic trap is a system of five rectangular electrodes, with a control alternating voltage applied to two of them (power electrodes are marked with numbers 2 and 4 in Fig. 1). The remaining three electrodes are grounded (marked with numbers 1, 3, 5 in Fig. 1). The length of the electrodes is 5 mm, the width of the power electrodes is 1 mm, and the width of the grounded electrodes is 2 mm. The spatial potential distribution around the trap electrodes can be described as

$$U(x,y,z,t) = \frac{1}{2\pi} V_0 \cos(\omega t) \sum_j f_j(x_{1j}, y_{1j}, x_{2j}, y_{2j}),$$
 (1)

where V_0 is the amplitude of the alternating voltage on the electrodynamic trap electrodes, ω is the frequency

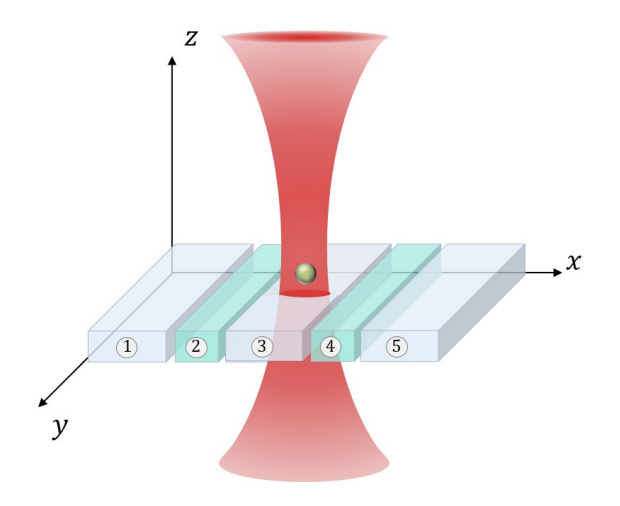


Fig. 1. Scheme of the electrodynamic trap

of the alternating voltage on the electrodes, f_j are the functions of spatial potential distribution over the j-th rectangular electrode with the coordinates of diagonal vertices $x_{1,i}$, $y_{1,i}$, $x_{2,i}$, $y_{2,i}$ [22]:

$$f_{j} = ^{-1} \left[\frac{(x_{1j} - x)(y_{1j} - y)}{z\sqrt{(x_{1j} - x)^{2} + (y_{1j} - y)^{2} + z^{2}}} \right] -$$

$$-^{-1} \left[\frac{(x_{1j} - x)(y_{2j} - y)}{z\sqrt{(x_{1j} - x)^{2} + (y_{2j} - y)^{2} + z^{2}}} \right] -$$

$$-^{-1} \left[\frac{(x_{2j} - x)(y_{1j} - y)}{z\sqrt{(x_{2j} - x)^{2} + (y_{1j} - y)^{2} + z^{2}}} \right] -$$

$$+^{-1} \left[\frac{(x_{2j} - x)(y_{2j} - y)}{z\sqrt{(x_{2j} - x)^{2} + (y_{2j} - y)^{2} + z^{2}}} \right].$$
 (2)

During modeling, the alternating voltage frequency was taken as $150\ kHz$, and the alternating voltage amplitude was $300\ V$.

The optical module of the hybrid trap is implemented on the principles of an optical tweezer using a focused laser beam with a Gaussian intensity profile I(x, y, z) in the form of [23]

$$I(x, y, z) = \frac{2P}{\pi W(z)^2} \exp\left[\frac{-2(x^2 + y^2)}{W^2(z)}\right], \quad (3)$$

where

$$W(z) = W_0 \sqrt{1 + [(z - h) / z_0]^2},$$

P is the laser radiation power, h is the height of the waist position above the electrode surface, $z_0 = \pi W_0^2 / \lambda$ is the Rayleigh length, λ is the laser radiation wavelength, W_0 is the width of the Gaussian beam waist.

The laser radiation is directed perpendicular to the trap surface. Both the case when the laser shines from bottom to top and when the radiation is directed from top to bottom are considered. The laser radiation wavelength was taken as $\lambda = 1064$ nm, and the waist position was set at a height of h = 1.2 mm from the trap surface. The width of the laser radiation waist was $\Omega_0 = 1000 \mu m$. The peak laser radiation power was considered to be $P_{\text{max}} = 16 \text{ W}$. It should be noted that the possibility of laser radiation propagation along the z axis through the trap electrodes can be physically achieved by using transparent thin-film electrodes. Previously, the possibility of creating fully transparent surface traps using thin films of indium and tin oxides (ITO) was successfully demonstrated [8,24]

Within the accepted approximations, from the side of optical radiation, two forces will act on the particle: the radiation pressure force F_{scat} along the laser radiation direction and the gradient force towards the intensity maximum, F_{grad} . In this case, the forces F_{scat} and F_{grad} can be written in the following form [2]

$$F_{scat}(z) =$$

$$= \hat{z} \frac{128\pi^5}{3} \frac{n_2^5 a^6}{c\lambda^4} \left(\frac{m^2 - 1}{m^2 + 2} \right)^2 I(x, y, z), \qquad (4)$$

$$F_{arad}(x, y, z) =$$

$$= \frac{2\pi n_2 a^3}{c} \left(\frac{m^2 - 1}{m^2 + 2} \right) \nabla I(x, y, z), \tag{5}$$

where n_1 and n_2 are the refractive indices of the particle material and the surrounding medium, respectively, $n_1 = 1.45$, $n_2 = 1$, $m = n_1 / n_2$, \hat{z} — unit vector along the axis z depending on the laser radiation propagation direction.

Taking into account all forces, the equations of motion of a charged nanoparticle when localized in air, considering viscous friction, will take the form

$$M\ddot{x} = -e\frac{\partial U(x, y, z, t)}{\partial x} - F_{grad, x} - 6\pi\mu a\dot{x}, \quad (6)$$

$$M\ddot{y} = -e\frac{\partial U(x, y, z, t)}{\partial y} - F_{grad, y} - 6\pi\mu a\dot{y}, \quad (7)$$

$$M\ddot{z} = -e \frac{\partial U(x, y, z, t)}{\partial z} - F_{grad, z} - F_{scat} - Mg - 6\pi\mu a \dot{z},$$
 (8)

where $F_{grad,\{x,y,z\}}$ are the components of the gradient force, M is the mass of the charged nanoparticle, e is the charge of the nanoparticle, μ is the dynamic viscosity of air.

Despite the fact that equations (6), (7) look the same, the described dynamics will differ significantly along the axes 0x and 0y. This difference will be related to the configuration of the electrodes under consideration. Since the electrodes are directed along the axis 0y, the electric potential gradient along the axis 0y is much smaller than along the axis 0x. In such a system, one can expect that the effects of breaking the symmetry of the effective potential will be more significant along the axis 0y [8].

Simulation of dynamics was carried out for the case of silicon dioxide nanoparticles with an average density $\rho = 2200 \text{ kg} / \text{m}^3$, radius a = 20 nm and surface charge equal to $e = 1.2 \cdot 10^2$ elementary charges. The dynamic viscosity of air was taken as $\mu = 18 \cdot 10^{-6} \text{ Pa} \cdot \text{s}$.

The positions of stable equilibrium can be determined by numerically solving the Cauchy problem for the system of differential equations (6), (8) with given initial conditions. Initial conditions were set taking into account the trap geometry features presented in Fig. 1. It was considered that the initial coordinates x and y correspond to the trap's middle point x(0) = 2 mm, y(0) = 2.5 mm, and the initial coordinate along the axis z is located at a distance within a random distribution $z(0) \in [1.2..1.5]$ mm from the trap surface. Initial velocities along the axes x, y and z were set randomly within the distribution $\dot{x}(0) \in [-2..2]$ mm/s, $\dot{y}(0) \in [-2..2]$ mm/s, $\dot{z}(0) \in [-2..2]$ mm/s, respectively. The solution was found using the

Runge-Kutta 4th order method with a variable integration step. Simulation was carried out in the time range $\tau \in [0..10^6]$, where $\tau = \omega t$.

3. DISCUSSION AND RESULTS

Figure 1 presents the simulation results of localization object dynamics at various laser radiation powers $P \in [-P_{max}...P_{max}]$ at $P_{max} = 16$ W. Negative values correspond to the direction of radiation propagation opposite to the gravity vector direction. In Figure 1a the dependence of particle stable equilibrium position coordinates along the 0z axis is plotted. In Figure 2b the dependence of particle stable equilibrium position coordinates along the 0y axis is plotted. When laser radiation is absent, the localization processes of charged particles are entirely determined by their interaction with the electrodynamic trap field. In this case, two stable equilibrium points are observed with coordinates along the 0y 3.2 mm and 1.8 mm at a height of 1.126 mm relative to the trap surface 1.126 mm. The presence of two stable equilibrium points is a consequence of the effective potential symmetry destruction in the electrodynamic trap, caused by the gravity force influence. This effect in surface electrodynamic traps was detailed in work [8]. When laser radiation impacts localization objects, a displacement of the nanoparticle position along the considered axes is observed. At laser radiation powers over 6.88 W when the laser radiation direction is from bottom to top and less than 12 W when the laser beam direction is from top to bottom, the bistable nature of the considered dynamic system is maintained. The bistability preservation is conditioned by the comparability of optical and electrical forces acting in the system.

At the same time, the action of the gradient force F_{grad} , which draws the nanoparticle into the area of maximum laser radiation intensity, leads to the convergence of stable equilibrium points along the axis 0y. An increase in the height of stable equilibrium points above the electrode surface is also observed. Several mechanisms immediately lead to this effect — drawing the nanoparticle into the waist under the action of F_{grad} , as well as leveling the effect of symmetry destruction of the effective potential when taking into account the potential energy of the nanoparticle in the optical field. When changing the radiation direction, all forces, except F_{scat} , retain their directions. The change

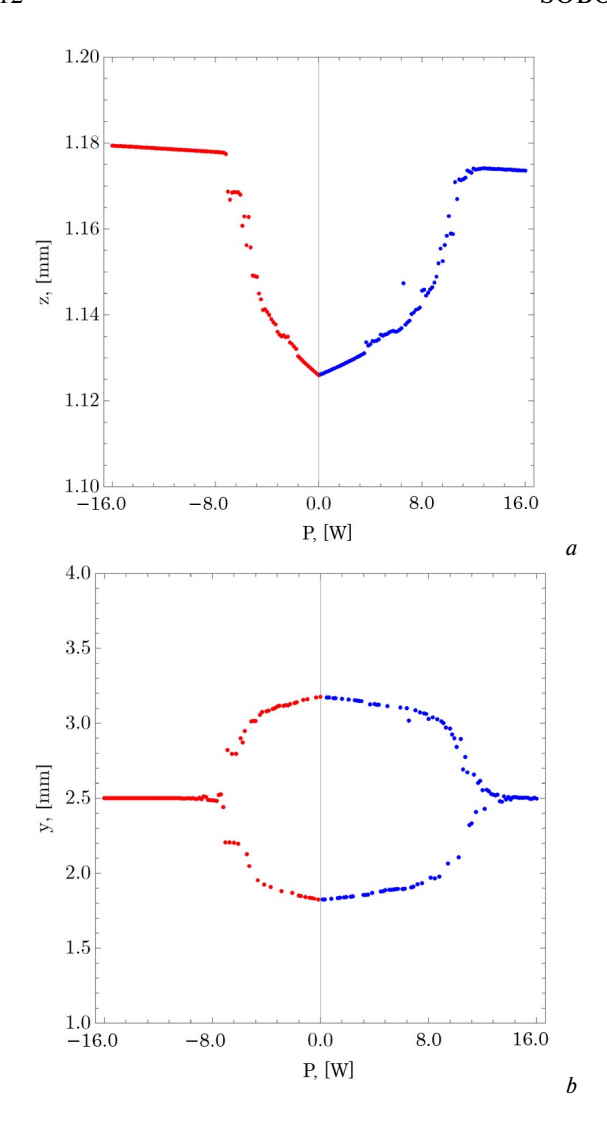


Fig. 2. Diagram of localization object dynamics depending on laser radiation power P. (a) — The dependence of the coordinates of the particle's stable equilibrium position along the axis 0z. (b) — Dependence of the coordinates of the particle's stable equilibrium position along the axis 0y

in the direction of the scattering force causes the asymmetry of the dependencies presented in Fig. 1.

At a radiation power below 6.88 W when the beam is directed from bottom to top and above 12 W when directed from top to bottom, the system transits to a state characterized by a single equilibrium position. In the case of powerful laser radiation, localization processes are almost entirely determined by the interaction with the optical module field, which is characterized by a single stable equilibrium position. The stable equilibrium point is located in the center of the trap, and its height above the electrode surface is determined by the power of laser radiation. The action of F_{scat} leads to a further rise

of the nanoparticle above the electrode surface when the radiation is directed from bottom to top and a decrease in the height of the localized nanoparticle when the radiation is directed from top to bottom.

Previously in the text, it was noted that the proposed hybrid trap configuration implementing the dynamics of a nanoparticle with a pitchfork bifurcation can be used as a platform for solving combinatorial optimization problems, which is equivalent to minimizing the Hamiltonian in the Ising model [14]. In the work [25], a computational scheme for finding the global minimum of the Ising Hamiltonian was proposed for a controlled dissipative system with bifurcation, based on a hybrid analog-digital representation of binary spins [12]. The scheme is implemented using the Lyapunov function gradient descent method, which is the sum of the analog Ising Hamiltonian and a single or double well potential. In [26], it was shown that the first non-zero stable states that become stable when changing the potential shape from a single well to a double well are associated with the global minimum of the Ising Hamiltonian. In such a computational scheme for solving combinatorial optimization problems, an analog version of the Ising Hamiltonian is used as a source of losses in an open dissipative system. In this case, the general equation describing the dynamics of a dissipative system with feedback for N analog generalized coordinates q_i , can be represented as follows

$$\frac{d^2q_j(t)}{dt^2} = -\frac{\partial}{\partial q_j} \left[\sum_j V_{\rm B}(q_j) + \beta V_I(\mathbf{q}) \right], \quad (9)$$

where $V_B(q_j)$ is a bistable effective potential, representing a function of time-averaged kinetic energy of fast oscillations taking into account all forces specified in equation (7);

$$V_I(\mathbf{q}) = -\sum_{j,l} \omega_{jl} q_j q_l$$

is analog form of the Ising Hamiltonian; β is coupling force between dynamic variables, $0 < \beta \ll 1$; ω_{jl} is the coupling matrix of dynamic variables, defining the conditions of the combinatorial problem and possessing the following properties:

$$\omega_{jl} = \omega_{lj}, \omega_{jj} = 0.$$

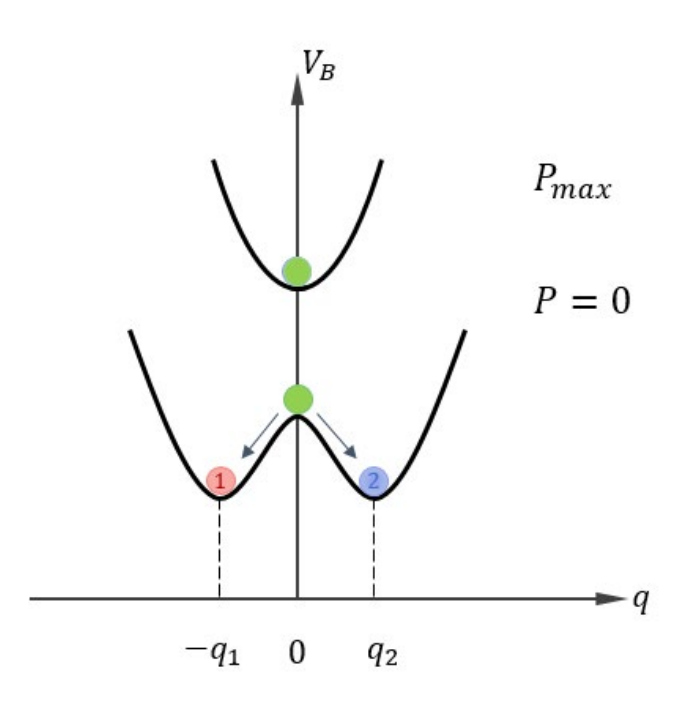


Fig. 3. Bistable potential of the optomechanical system

In the general case, the potential V_B can be represented as

$$V_B(q_j) = -1/2\alpha q_j^2 + 1/4q_j^4,$$

and the dynamics equations at $\beta = 0$ take the form characteristic of a bifurcation system [25]:

$$\ddot{q}_j = \alpha q_j - q_j^3, \tag{10}$$

where α is the control parameter. The system has one stable state $q_j = 0$, when the control parameter has a value less than critical (single well potential) and two stable states when the value α is greater than critical (double well potential), which is schematically shown in Fig. 3. In the case when $\beta \neq 0$, the dynamics equations will take the form

$$\ddot{q}_j = \alpha q_j - q_j^3 - \beta \sum_l \omega_{jl} q_l. \tag{11}$$

Equations (11) describe the dynamics of N-partial system, where parameter α determines the gain, and the last term obtained from the analog Ising Hamiltonian describes the losses in the system. With continuous increase in gain, the system tends to a state with the least losses, which corresponds to finding the minimal energy of a given Ising

Hamiltonian. To use the optomechanical system considered in this work as a physical platform for solving combinatorial problems, the approach proposed in works [12,26] can be implemented. This approach is based on an analog-digital representation of binary spins and their time multiplexing. With this approach, spin values are determined using the nonlinear dynamics of the optomechanical system for each of the N spins sequentially with time separation, and the calculation of inter-spin interaction contained in the Ising Hamiltonian, which implies the implementation of vectormatrix multiplication according to the conditions of the combinatorial problem, is carried out using digital methods and devices. In this case, in the optomechanical system, the control parameter is the laser radiation intensity, and spin encoding $\sigma_i = \pm 1$ is based on determining the particle position along the axis 0y, in the context of the described formalism $\sigma_i = q_i/|q_i|$. A more detailed description of using the proposed optomechanical system as a platform for solving combinatorial problems will be considered in a separate work.

4. CONCLUSIONS

In this work, the features of the localization process for charged dielectric nanoparticles in hybrid traps are examined. A configuration of a hybrid trap is proposed, consisting of a surface electrodynamic trap with transparent electrodes and an optical dipole trap. The surface trap is implemented using five flat rectangular electrodes. A focused laser radiation with a Gaussian intensity distribution is used as the dipole trap. The calculations assumed that the laser radiation is directed normally to the surface of the electrodynamic trap. Dynamics simulation was carried out for charged silicon dioxide nanoparticles with a hydrodynamic radius of 20 nm. Simulation shows that in the absence of laser radiation, two stable equilibrium positions are formed. When exposed to focused laser radiation, the stable equilibrium points converge up to their complete merger. The change in coordinates of the stable equilibrium points is explained by the action of the gradient force, which contributes to drawing transparent nanoparticles into the region of the highest laser radiation intensity. It should be noted that the change in stable equilibrium coordinates is achieved without changing the laser radiation direction or the relative position of trap elements. This work shows that depending on the laser radiation direction, the bifurcation point is observed at different values of the control parameter — laser radiation power. Moreover, an asymmetry of dependencies of stable equilibrium point coordinates on laser radiation power is observed when considering the radiation propagation direction. The asymmetry of dependencies is explained by the change in the direction of the scattering force acting along the laser radiation direction. Thus, the system is characterized by a controlled bifurcation of particle equilibrium positions. The proposed hybrid trap configuration can become a new platform for implementing a new type of Ising optomechanical machine.

FUNDING

The study was carried out with financial support from the Russian Science Foundation grant No. 22-42-05002

REFERENCES

- 1. P. Polimeno, A. Magazzu, M. A. Iati et al., *Optical Tweezers and Their Applications*, J. of Quantitative Spectroscopy and Radiative Transfer **218**, 131 (2018).
- 2. Z. Liu and D. Zhao, Radiation Forces Acting on a Rayleigh Dielectric Sphere Produced by Highly Focused Elegant Hermite-cosine-Gaussian Beams, Optics Express 20, 2895 (2012).
- 3. N. Viana, A. Mazolli, M. Neto et al., *Absolute Calibration of Optical Tweezers*, Appl. Phys. Lett. **88**, 131110 (2006).
- **4.** G. P. Conangla, R. A. Rica and R. Quidant, *Extending Vacuum Trapping to Absorbing Objects with Hybrid Pauloptical Traps*, Nano Lett. **20**, 6018 (2020).
- J.-M. Cui, S.-J. Sun, X.-W. Luo et al., Cold Hybrid Electrical-Optical Ion Trap, arXiv preprint arXiv:2306.10366 (2023).
- 6. J. Pérez-Ríos and C. Greene, *Reactivity in Ion-neutral High Density Medias*, EPJ Web of Conferences **113**, 02004 (2016).
- 7. J. Kwolek, D. Goodman, B. Slayton et al., *Measurement of Charge Exchange Between Na and in a Hybrid Trap*, Phys. Rev. A **99**, 052703 (2019).
- 8. D. Shcherbinin, V. Rybin, S. Rudyi et al., *Charged Hybrid Microstructures in Transparent Thin-film Ito Traps: Localization and Optical Control*, Surfaces **6**, 133 (2023).

- 9. S. Rudyi, A. Ivanov, and D. Shcherbinin, *Fractal Quasi-coulomb Crystals in Ion Trap with Cantor Dust Electrode Configuration*, Fractal and Fractional 7, 686 (2023).
- U. Tanaka, M. Nakamura, K. Hayasaka et al., Creation of Double-well Potentials in a Surfaceelectrode Trap Towards a Nanofriction Model Emulator, Quantum Science and Technology 6, 024010 (2021).
- 11. Y. Shi, H. Zhao, L. K. Chin et al., *Optical Potentialwell Array for High-selectivity, Massive Trapping and Sorting at Nanoscale*, Nano Lett. **20**, 5193 (2020).
- **12**. T. Inagaki, Y. Haribara, K. Igarashi et al., *A Coherent Ising Machine for 2000-node Optimization Problems*, Science **354**, 603 (2016).
- **13**. S. Tanaka, Y. Matsuda and N. Togawa, *Theory of Ising Machines and a Common Software Platform for Ising Machines*, 2020 25th Asia and South Pacific Design Automation Conference (ASP-DAC) 659 (2020).
- **14**. A. Lukas, *Ising Formulations of Many NP Problems*, Frontiers In Physics **2**, 74887 (2014).
- 15. N. Mohseni, P. L. McMahon and T. Byrnes, *Ising Machines as Hardware Solvers of Combinatorial Optimization Problems*, Nat. Rev. Phys. 4, 363 (2022).
- **16**. A. Marandi, Z. Wang, K. Takata et al., *Network of Time-multiplexed Pptical Parametric Oscillators as a Coherent Ising Machine*, Nature Photonics **8**, 937 (2014).
- 17. Y. Rah, Y. Jeong, S. Han et al., *Low Power Coherent Ising Machine Based on Mechanical Kerr Nonlinearity*, Nature Photonics **130**, 073802 (2023).
- **18**. S. Razmkhah, M. Kamal, N. Yoshikawa et al., *Josephson Parametric Oscillator Based Ising Machine*, Phys. Rev. B **109**, 014511 (2024).
- **19**. H. Du, *Mie-scattering Calculation*, Appl. Opt. **43**, 1951 (2004).
- **20**. E. J. Davis, Periasamy and Ravindran, *Single Particle Light Scattering Measurements Using the Electrodynamic Balance*, Aerosol Science and Technology **1**, 337 (1982).
- **21**. M. G. House, *Analytic Model for Electrostatic Fields in Surface-electrode Ion Traps*, Phys. Rev. A **78**, 033402 (2008).
- **22**. N. N. Mirolyubov, M. V. Kostenko, M. L. Levinshtein et al., *Methods for Calculating Electrostatic Fields*, Vysshaya Shkola, Moscow (1963), p.4. (in Russian)
- **23**. Saleh, Bahaa, Teich et al., *Fundamentals of Photonics*, John Wiley and Sons (2019).
- **24**. D. P. Shcherbinin, V. V. Rybin, S. S. Rudyi et al., *Transparent Surface Radio-frequency Trap*, SPIE Future Sensing Technologies **12327**, 359 (2023).

- **25**. T. Leleu, U. Utsunomiya and K. Aihara, *Combinatorial Optimization Using Dynamical Phase Transitions in Driven-dissipative Systems*, Phys. Rev. 022118 (1995).
- **26**. F. Böhm, G. Verschaffelt and G. Van der Sande, *Poor Man's Coherent Ising Machine Based on Optoelectronic Feedback Systems for Solving Optimization Problems*, Nat. Commun. 10, 3538 (2019).